한국지진공학회 논문집 | 제11권 제5호 (통권 제57호) | 2007년 10월, pp. 23~32

Bending behavior of shape memory alloy bar and its application of seismic restrainers for bridges

형상기억합금의 휨거동 및 교량변위제어장치적용 연구

최은수[1] · 박주남[2] · 김학수[3] · 이도형[4]

Choi, Eun-Soo · Park, Joo-Nam · Kim, Hak-Soo · Lee, Do-Hyung

국문 요약 >> 본 논문은 형상기억합금 바의 휨 거동 특성 파악하기 위하여 여러 가지의 휨 거동 실험을 수행하였으며, 형상기억합금 바의 휨 거동 분석을 통하여 지진 시에 적용 가능성을 규명하는데 목적이 있다. 이를 위해 단순 휨 및 이중 휨 실험을 재하속도 및 최대변위를 변수로 수행하였다. 힘-변위 곡선에서 추정한 재하 및 제하 시의 강성이 추정되었으며, 등가의 감쇠비도 각 실험결과에서 추정되었다. 단순 휨에서 형상기억합금 바는 32 mm 변위 이후에 강성증가현상을 나타냈으며, 이것은 SIM(Stress-Induced-Martensite) 현상에 의해서 발생하는 것으로 추정된다. 재하속도의 증가는 형상기억합금 휨 강성 증가에 영향을 주지 않는 것으로 나타났다. 이중 휨 거동에서 형상기억합금 바는 단순 휨에 비해 강성이 약 5배정도 크게 나타났으며, 감쇠비는 유사하게 나타났다. 휨 거동의 형상기억합금 바를 지진변위 제어장치로 사용하여 3경간 단순지지 교량에 적용하여 지진해석을 수행하였다. 이러한 지진변위 제어장치는 매우 효과적인 것으로 나타났으며, 실용적인 것으로 판단된다. 본 논문의 의미는 형상기억합금 바의 휨 거동에 대한 기초 지식을 제공하는데 있다.

주요어 형상기억합금, 교량, 지진변위제어장치, 휨 거동

ABSTRACT >> The goal of this study is to perform several bending tests on a shape memory alloy bar and to analyze the characteristics of the bending behavior. The other goal is to verify the seismic performance of an SMA bar bending application. Single and double bending tests were conducted with varying loading speeds and maximum displacement. The loading and the unloading stiffness were estimated from the force-displacement curves and the equivalent damping ratio of each test was also assessed. In single bending, the SMA bar showed the stiffness hardening after the displacement of 32 mm. It is assumed that this phenomenon is due to the stress-induced-martensite hardening. The increasing loading speed did not influence on the stiffness of the single bending SMA bar. The stiffness of the double bending bar is about 5 times of that of the single bending. This study introduced a seismic application of SMA bending bars as seismic restrainers for bridges and showed its practicality. SMA bars in bending are used for seismic restrainers in a three-span-simply-supported bridge. They showed the effectiveness to reduce the responses of the bridge and the applicability for a seismic restrainer. The significance of this study is to provide basic knowledge of SMA bending and its seismic applications.

Key words Shape Memory Alloy, Bridges, Seismic Restrainer, Bending Behavior

1. Introduction

Shape memory alloys (SMA) show unique mechanical behaviors, such as shape memory effect and superelastic effect, and, thus, have potential for use in engineering application. One of the most fervently researched topics related to SMA, in civil engineering, is the seismic retrofit of bridges and buildings. The seismic applications of SMA for bridges are concentrated on dampers or restrainers; the shape memory effect is good for seismic dampers to dissipate seismic energy and the superelastic effect which allows large deformations to recover without residual deformation, is valuable for restrainers. In those applications, SMAs are activated in tension, compression, or both. Therefore, experimental tests on SMAs usually consist of tensile or compressive tests to support their applications.

Grasser and Cozzarelli (1991) developed a one-dimensional constitutive model to describe the force-deformation behavior of Nitinol (Ni-Ti alloy) SMA varied due to loading

[1] 정회원·홍익대학교 토목공학과 조교수
(대표저자: eunsoochoi@hongik.ac.kr)
[2] 정회원·한국철도기술연구원 철도구조물연구팀 선임연구원
[3] 호남대학교 토목공학과 부교수
[4] 정회원·배재대학교 공과대학 건설환경철도공학과 부교수
(교신저자: dohlee@pcu.ac.kr)

본 논문에 대한 토의를 2007년 12월 30일까지 학회로 보내 주시면 그 결과를 게재하겠습니다.

(논문접수일 : 2007. 1. 30 / 심사종료일 : 2007. 7. 5)

frequency and verified the model with experimental work. Dolce et al. (2000) developed a seismic damper for civil structures using SMA wires. The basic concept of their damper is the combination of martensite SMA wires for energy dissipation and austenite wires for recentering, and the effectiveness of the device was proved through experimental works. DesRoches and Delemont (2002) used SMA bars as restrainers instead of steel cable in bridges. They showed that the SMA bars are more effective to restrain relative deck displacement than the conventional steel cable restrainers. Wilde et al. (2000) also used SMA bars combining with elastomeric bearings for bridges. The SMA system was verified as an effective device to control relative deck displacement.

The above studies of seismic dampers or restrainers using SMA wires or bars were based on the tension or compression or both behavior. However, the bending of SMA bars may be more effectively used as dampers or restrainers in several cases. For example, Ocel et al. (2004) used the bending of SMA bars to dissipate seismic energy on the connection of beam-column in a steel frame. Also, Adachi and his colleagues (1999) attached an SMA plate as a damper or a restrainer to improve seismic bridge response. Although Ocel (2004) and Adachi (1999) used the bending behavior of SMA plates or bars, they did not show the mechanical bending behavior of the SMA members.

Therefore, the understanding of the bending behavior of SMA bars or plates was not addressed in their studies. This study performed single and double bending test of an SMA bar and discussed the mechanical bending behavior of the bar. Based on the results of the experimental tests, an analytical model of the SMA bending bars, which is used to evaluate the effectiveness of the restrainer of SMA bending bars in multi-span simply supported bridges. Also, this study suggests a basic understanding of SMA bars in bending and illustrated how to apply bending behavior in seismic applications.

2. Bending Test of SMA Bar

The 25.4 mm diameter Nitinol shape memory alloy rod shown in Figure 1 was tested. The bar had a length of 152 mm and was 25% cold-worked. The specimen was threaded at the ends and vacuum annealed at 450°C for 60 minutes, followed by water quenching.

To conduct a bending test of a bar, a force at the top of a bar should be applied perpendicularly to the bar and the bottom of the bar is fixed. The top of the bar where a force is applied should have special boundary conditions for single and double bending; 1) lateral movement and rotation are permitted for a single bending and 2) lateral movement is permitted but restrained is the rotation of the top for a double bending. For this purpose, a specially manufactured ball, piston, and cylinder, which are shown in Figure 2, were used. Figure 3 shows the combined shape of the SMA bar and the ball or piston. In the combination of the ball and the cylinder, the ball permits the rotation of the SMA bar while the cylinder is moving laterally. In the same manner, in the docking of the piston and the cylinder, the piston restrains the rotation of the top. In bending tests, two circular plates were located between the top and the bottom plate of the test machine to prevent the contact of the ball or the piston to the cylinder's bottom. This set up confirms that there is not any compressive force on the SMA bar during its bending. Figure 3(b) shows the whole set up and the bended shape of an SMA bar in single and double bending test. In the bending tests, the displacement

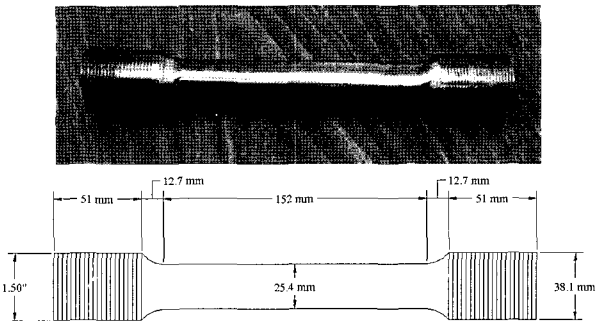

〈Figure 1〉 Superelastic SMA bar (Up: Photo, Down: Schematic)

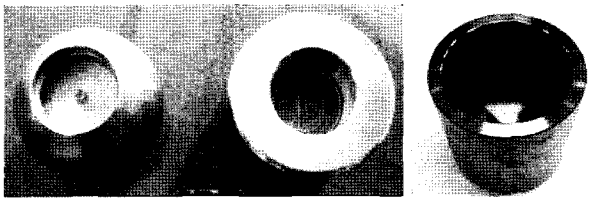

〈Figure 2〉 A ball, a piston and a cylinder to realize boundary conditions

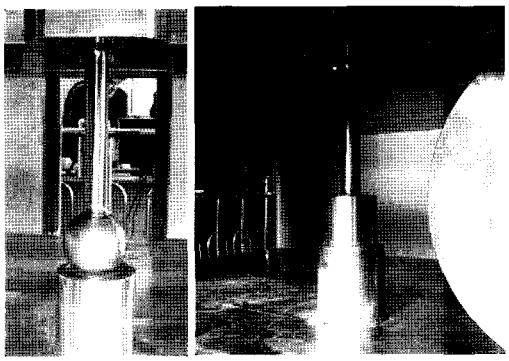

(a)

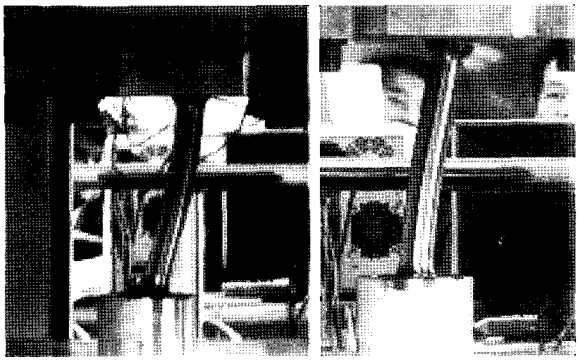

(b)

〈Figure 3〉 Test set up and bending shape of a SMA bar; (a) Docking of the ball and the piston to the cylinder, (b) SMA bar's single and double bending shape

control was performed. In the single bending test, the maximum displacements were varied form ±10 mm to ±40 mm with increasing ±5 mm. In all tests, 3 cycle loadings were applied.

At the displacement of 40 mm, the tensile strain of the SMA bar at the fixed point was calculated as 6% over which the bar could be damaged (DesRoches et al., 2004). Therefore, the maximum displacement did not exceed the 40 mm. The loading speeds were 0.025 Hz for quasi-static loading and 0.5 Hz for dynamic loading. Since DesRoches et al. (2004) mentioned the strength hardening of an SMA bar in tension due to the loading speed, this study checked wetherr this phenomenon happens in bending of SMA bars. In double bending tests, the maximum displacements are varied from ±5 mm to ±20 mm with increasing ±5 mm.

The machine used for these tests has the capacity of 2,000 kN in horizontal and ±1500 kN in vertical direction. The maximum strokes are ±250 mm in horizontal and 200 mm in vertical direction. The maximum loading speed is 130 mm/sec.

3. Experimental Results and Discussion

The test results are shown in Figures 4-6. From the hysteretic curves, the loading and the unloading stiffness and the equivalent damping ratio are estimated. In each figure, the loading stiffness and the equivalent damping ratio are shown up.

In the single bending tests, the loading stiffness was close to the unloading one. The dynamic test results were similar to those in the quasi-static tests. The strength increment appeared in a tensile test of an SMA bar with a dynamic loading that was not observed in the bending test. In a tensile test, the tensile stress was developed uniformly for the whole SMA bar. Thus, a large area can be exposed to a high stress. However, in the bending test, the developed high tensile stress was concentrated on the small area at the fixed point of the SMA bar. The reason of the strength increment is assumed to be that the heat generated from the atomic friction is not released due to a high speed loading and, then, the captured heat makes an SMA bar harder. Since this phenomenon appeared in a small area in a bending test, the strength-increment effect was negligible.

In Figure 4(f), the hardening effect is observed at the displacement of 32 mm. Its cause is assumed to be the Stress-Induced-Martensite (SIM) hardening which is developed at the tensile strain of 6% (DesRoches et al., 2004). The SIM hardening indicates that the tensile strain at the fixed point exceeds 6% and is close to the maximum strain of 8% at which the specimen could be failed.

The estimated loading and unloading stiffness and equivalent damping ratios are arranged in Table 1 and 2 for the single bending tests of the quasi-static and dynamic loads, respectively. The average loading and unloading stiffness are 0.223 kN/mm and 0.212 kN/mm. The unloading and the loading stiffnesses are much the same to the displacement of 25 mm; however, the unloading stiffness was less than the loading ones after the displacement of 30 mm. This is assumed to be caused by SIM hardening at the fixed point of the specimen. The average damping ratio is 6.7% that is larger 67% than that in tension (DesRoches et al., 2004).

In the single bending tests with dynamic loadings, the

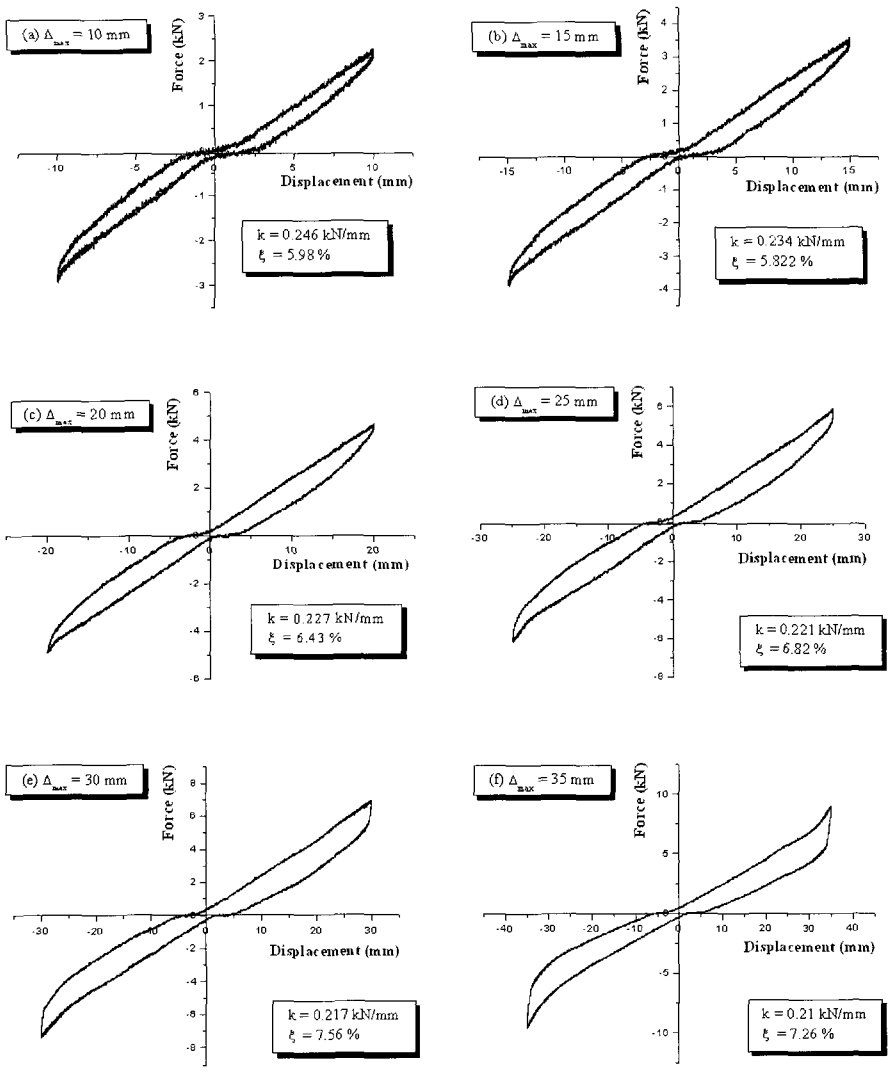

〈Figure 4〉 Force-displacement curves of the single bending with a quasi-static loading (loading speed= 0.025 Hz)

〈Table 1〉 Loading and unloading stiffness and equivalent damping ratio of the single bending tests with quasi-static loadings

Max. displacement (mm)	Loading stiffness (kN/mm)	Unloading stiffness (kN/mm)	Damping ratio (%)	Residual deformation (mm)
10	0.246	0.255	5.98	1.755
15	0.234	0.238	5.82	2.808
20	0.227	0.233	6.43	4.388
25	0.221	0.231	6.82	5.867
30	0.217	0.173	7.56	8.249
35	0.210	0.168	7.26	10.61
40	0.207	0.137	7.06	12.79
Average	0.223	0.212	6.70	

〈Table 2〉 Loading and unloading stiffness and equivalent damping ratio of the single bending test with dynamic loadings

Max. displacement (mm)	Loading stiffness (kN/mm)	Unloading stiffness (kN/mm)	Damping ratio (%)	Residual deformation (mm)
10	0.209	0.279	5.37	2.006
20	0.202	0.220	7.10	4.889
30	0.196	0.189	7.67	8.425
40	0.223	0.138	6.64	12.787
Average	0.208	0.207	6.69	

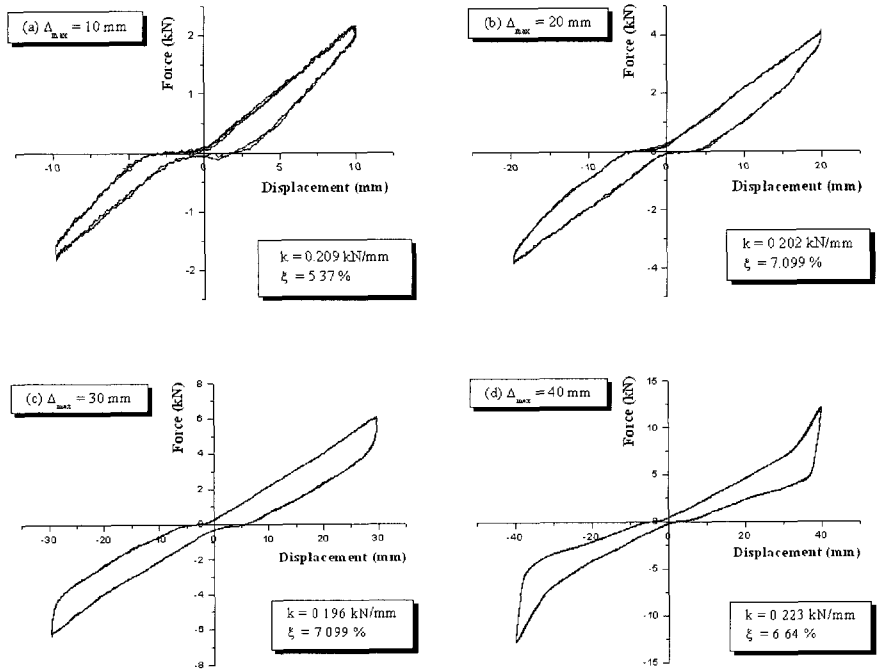

〈Figure 5〉 Force-displacement curves of the single bending with a dynamic loading (loading speed= 0.5 Hz)

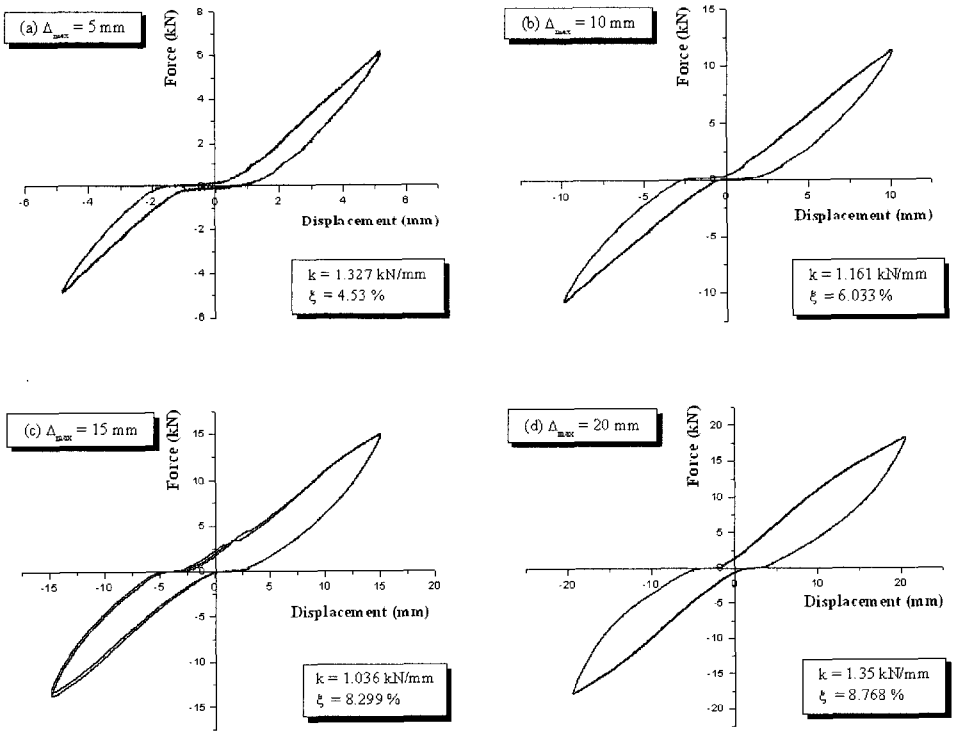

〈Figure 6〉 Force-displacement curves of the double bending with a quasi-static loading (loading speed= 0.025 Hz)

average loading and unloading stiffness are 0.208 kN/mm and 0.207 kN/mm, and the average damping ratio is 6.69%. Although the loading stiffness with dynamic loadings is less than that of the quasi static loadings, the general trend of the double bending behavior is similar to the single bending.

The double bending test results are listed in Table 3. The average loading and unloading stiffness are 1.104 kN/mm and 1.263 kN/mm that are approximately 5 times larger than those from the single bending. The average

〈Table 3〉 Loading and unloading stiffness and equivalent damping ratio of the double bending test with quasi-static loadings

Max. displacement (mm)	Loading stiffness (kN/mm)	Unloading stiffness (kN/mm)	Damping ratio (%)	Residual deformation (mm)
10	1.327	1.459	4.53	1.038
20	1.161	1.343	6.03	2.501
30	1.036	1.167	8.30	4.599
40	0.893	1.083	8.77	6.367
Average	1.104	1.263	6.91	

damping ratio is 6.91% which is close to that of the single bending. In the single bending, the loading and the unloading stiffness are similar before the SIM hardening is developed. However, in double bending, the unloading stiffness is larger from 9% to 17% than the loading stiffness.

The residual deformations after the bending increase with increasing the displacement; which means that the recentering capability decreased with large bending displacement. The residual deformations of the double bending are larger than those of the single bending since the developed strains of the double bending are larger than those of the single bending.

4. Seismic Applications of SMA Bending

Use of SMA in bending appears to have many benefits that could be applied to their use as seismic mitigation devices. The recentering capability and increased damping could all improve the response of bridges in earthquakes. In use of SMA bars in tension, compression, or both, a connection would have to be designed that would allow an SMA bar to be used in tension and compression without buckling, and which would still allow thermal movement of the bridge. However, such a connection is not easy to be realized. For example, Wilde's study requires 2 m long SMA bar in tension and compression to mitigate the seismic response of a bridge in transverse direction (Wilde et al., 2000). Therefore, any device is necessary to prevent the bar's buckling.

When the bending of SMA bars is used in seismic applications, the bars are located perpendicular to the developed seismic force due to an earthquake in bridges. This makes their installation easier. With a lock-up device, the thermal expansion of bridges can be absorbed easily shown in Figure 7(a); the device could be a

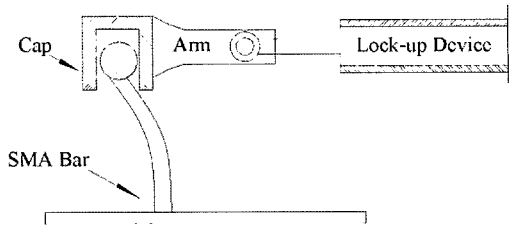

(a) SMA seismic restrainer

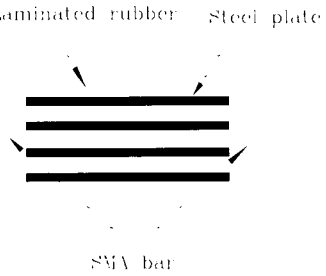

(b) Elastomeric bearing with SMA bars

〈Figure 7〉 Applicable seismic devices with SMA bars

damper or seismic restrainer during an earthquake. Also, SMA bars can be used in an elastomeric or frictional bearing to increase recentering capability and damping to compensate the weak points of conventional elastomeric or frictional bearings as shown in Figure 7(b). An elastomeric bearing has relatively small damping and a frictional bearing does not any recentering capability. The SMA bars in bridge bearings also can provide the resistance to up-lifting force.

5. Analytical Model of SMA Bar Bending and Seismic Analysis

An analytical model of the SMA single bending tested above is developed using bilinear model. The initial stiffness is 2.16 kN/mm and the post yielding stiffness is 0.216 kN/mm. Also, the yielding force is 0.5 kN. The bilinear model of the SMA bar bending matches approximately with the bending behavior. The behavior of the SMA bending is so variable according to the deformation

that it is hard to develop its exact analytical model. Figure 8 compares the analytical model of the SMA bending bar to its experimental results in single bending.

A three span simply supported steel bridge as shown in Figure 9(a) is modeled for this study; which is typically found in the central and southeastern United States (Choi, 2002). The decks of the bridges are supported by an array of fixed and expansion steel bearings and each deck has 11 steel girders. The bridges consist of several components such as columns, abutments, steel bearings, foundations, and superstructures; some of them, particularly columns and bearings, exhibit highly nonlinear behavior. Therefore, two-dimensional nonlinear analytical model of the bridge in longitudinal direction is developed using DRAIN-2DX nonlinear analysis program (Prakash et al. 1992). The superstructure is usually expected to remain linear under longitudinal earthquake motions so that it is modeled using a linear element. In the bridge model, abutments are modeled with multiple line nonlinear behavior. Columns consist of 22 fiber elements for unconfined and confined concrete and reinforcements. The pile foundations are modeled with linear springs for horizontal and rotational direction (Choi, 2002).

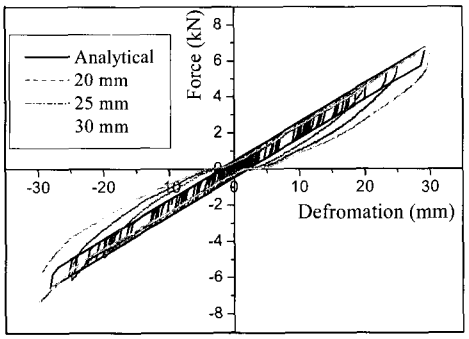

〈Figure 8〉 Comparison of analytical model and experimental results of the SMA bending bar

The SMA bars are installed perpendicular to the deck beside expansion bearings as shown in Figure 9(b). The

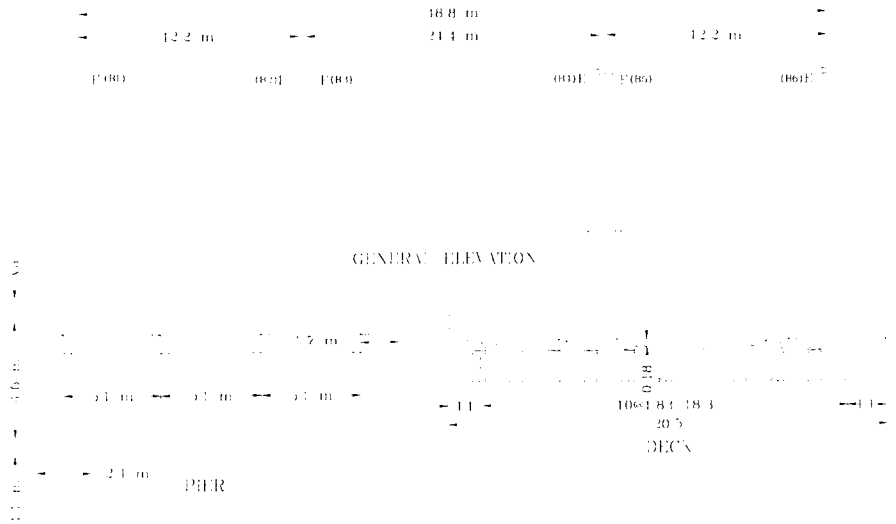

(a) Bridge configuration

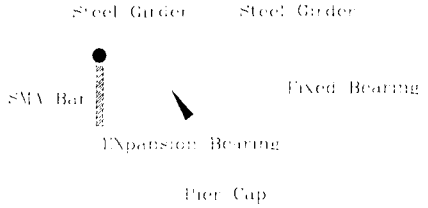

(b) SMA bar installing

〈Figure 9〉 Three span simply supported steel bridge configuration (△: fixed bearing; ○: expansion bearing) and installing of an SMA bar on a pier cap.

bottom of an SMA bar is fixed at the top of a pier cab or an abutment and the top of the bar is permitted to translational and rotational movement. Therefore, the bar is experienced single bending behavior during an earthquake and such as a seismic restrainer. Since the SMA bars are installed by the side of every expansion bearing, the bridge system is connected together from the left abutment to the right one. Conventional cable restrainers use only the pulling capacity of abutments (DesRoches and Fenves, 1997), however, the SMA bending bar can use the both capacity of pulling and pushing action of abutments. In an abutment, the stiffness and strength in pushing action is much larger than those in pulling action since a soil pressure is developed in the back of an abutment during in pushing action. In the analytical model of the abutment in Figure 10, the initial stiffness in active (pulling) action is 212 kN/mm and the yield deformation is 7.62 mm. Also, the elastic stiffness in passive (pushing) action is 669 kN/mm and the elastic range is 14.6 mm. Thus, the pushing action is about 3 times stiffer than the pulling action in the abutment and the strength is approximately 6 times larger in pushing action than that in pulling action. 10 artificial ground motions generated for New Madrid Seismic Zone are used for seismic analysis of the bridge (Wen and Wu, 2001). Their occurring probability is 2% in 50 years and, thus, the recurrence period is 2475 years. Figure 11 shows the averaged response spectrum of the 10 ground motions and the average± the standard deviation. 2 or 4 SMA bars as a restrainer are installed at the expansion bearing place of each girder. After this, SMA-2 and SMA-4 represent the 2 and 4 SMA bars restrainer, respectively.

The analytical results of the as built and the retrofitted bridge are compared to discuss the effectiveness of the restrainer of the SMA bending bars. The interesting responses are column's drift ratio of the top displacement divided by the column length, bearing deformation, opening, and abutment deformation. Table 4 shows the

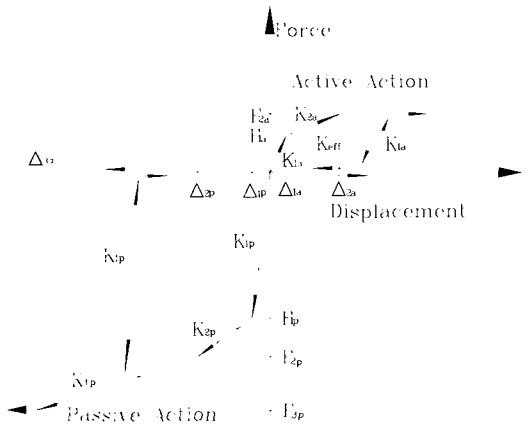

〈Figure 10〉 Analytical model of an abutment

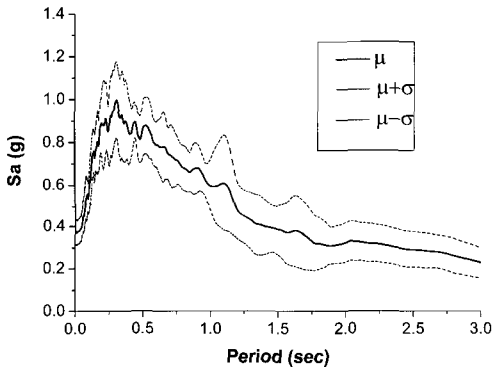

〈Figure 11〉 Average response spectrum of 10 ground motions

〈Table 4〉 Averages and standard deviations of interesting responses

Type	Response	Drift ratio (%)		Fixed bearing deform. (mm)			Opening (mm)			Abutment deformation (mm)			
		Col1	Col2	Fx1	Fx2	Fx3	Op1	Op2	Op3	Ab1+	Ab1-	Ab2+	Ab2-
As-Built	μ	0.750	0.604	11.8	0.909	0.814	52.6	9.42	37.5	4.01	3.12	0.612	1.13
	σ	0.116	0.066	3.72	0.577	1.21	7.47	1.86	5.77	0.807	0.429	0.075	1.21
	μ+σ	0.866	0.67	15.52	1.486	2.024	60.1	11.3	43.3	4.817	3.549	0.687	2.34
SMA-2	μ	0.687	0.547	11.0	0.748	0.253	45.3	9.59	32.9	4.58	3.03	1.33	0.744
	σ	0.110	0.060	3.46	0.317	0.238	7.64	1.17	4.46	0.873	0.399	0.158	0.772
	μ+σ	0.797	0.607	14.46	1.065	0.491	52.9	10.8	37.4	5.453	3.429	1.488	1.516
SMA-4	μ	0.617	0.496	9.23	0.640	0.123	38.7	8.57	28.8	4.80	2.82	1.88	0.679
	σ	0.089	0.059	3.94	0.157	0.035	5.85	1.29	3.83	0.870	0.455	0.222	0.272
	μ+σ	0.706	0.555	13.17	0.797	0.158	44.6	9.86	32.6	5.67	3.275	2.102	0.951

* Col1 & Col 2 : the first column from left and the second
* Fx1, Fx2, & Fx3 : Fx1 is the fixed bearing on the left abutment, FX2 is the one on the first pier, and FX3 on the second pier.
* Op1, Op2, & Op3 : Op1 represents the opening between the first and the second deck from left. Op2 does between the second and the third deck. Op3 does between the third deck and the right abutment.
* Ab1+,Ab1-,AB2+,Ab2-: Ab1 is the abutment in the left and (+) represents the pulling action and (−) does the pushing action.

averages and the standard deviations of interesting responses. In this study, the values of the average+ standard deviation will be compared. For the SMA-2 case, the column drift ratios are reduced by 8.0 and 9.4% of the first (Col 1) and the second pier (Col 2) from left. The fixed bearing deformation of Fx1 decreases by 6.8%. The maximum opening is reduced from 60.1 mm to 52.9 mm; the opening is a very critical response related to the unseating of bridges. However, the abutment deformations in pulling action increase with SMA bars. Especially, the right abutment (Ab2) pulling deformation increases by 116% of that of the as-built. In the as-built bridge, since expansion bearings are located on the abutment, their pulling force is not large enough to generate large deformation in the abutment. However, the deformation of 1.52 mm in pulling action is much less than the capacity of 7.62 mm. Therefore, the abutment is still in elastic range. The SMA bars on the abutment (Ab2) also add more force to the pushing action. However, the pushing deformation of the abutment decreases by 35.2% by the SMA-2 case. The SMA bars restrict the decks' movement and, thus, reduce the pounding force on the abutment. A pounding in an abutment generates a large deformation in pushing action and local damage such as cracks. For the case of SMA-4, all responses are improved more than the case of SMA-2 except the pulling deformation of the abutments. In the left abutment (Ab1), the pulling deformation with SMA-4 reaches 5.67 mm which is 74.4% of the elastic range of 7.62 mm. Therefore, the abutment is still safe from the pulling deformation. The SMA-4 reduces the maximum column drift by 18% and the opening by 26%. The noticeable response is the pushing deformation of the right abutment (Ab2). Its deformation reduces from 2.34 mm to 0.951 mm with SMA-4, which means that the SMA-4 prevents the pounding on the abutment successfully.

In this study, SMA bars in bending shows the effectiveness to protect bridges from earthquakes. Also, SMA bars in bending can be installed easier on bridges than SMA bars in tension or compression. However, the stiffness of SMA bars in bending is less than that in tension. It is necessary to use the SMA bar of high Young's modulus for the bending applications. SMA's Young's modulus varies from 20 to 80 GPa. The bar in this study has 28 GPa in tension (DesRoches et al., 2004). If the SMA bars of 80 GPa are used for this case, the number of bar or the cross-section area can be reduced by 2.8 times.

6. Conclusions

This study conducted several bending tests of a superelastic SMA bar and discussed the results of single and double bending with varying loading speed and maximum displacement. From the force-displacement curves of the single bending, the loading and the unloading stiffness were estimated and they showed similar values. The equivalent damping ratio is 6.7% averagely which is larger 67% than that in tension. Thus, it can say that the bending has more energy dissipation capacity. The loading speed can not change the single bending behavior of the specimen significantly different from the behavior in tension. The loading stiffness of the double bending is approximately 5 times larger than that of the single bending. Thus, the double bending is more applicable to restrain seismic displacement of bridges, however, it has smaller moving tolerance comparing to the single bending. The SIM hardening was also observed in bending as the same as in tension. The stiffness increment due to SIM hardening probably would be helpful to prevent unseating of bridge decks.

It is found that SMA bars in bending restraint the columns' movement and prevent poundings on abutments. Therefore, they can reduce the probability of the damage on bridge components such as columns, fixed bearings, and openings. However, SMA bars in bending increase the pulling deformation of abutments. Considering this point, the design of SMA bars in bending for a bridge depends critically on the pulling capacity of abutments.

As Wilde mentioned in his study, a long SMA bar in tension and compression needs some additional method to install stably and prevent buckling. The application of SMA bars in bending is more practical and easily combined with other devices.

Acknowledgement

This work was supported by the Hongik University new faculty research support fund. The authors would

like to acknowledge the financial support from Hongik University.

Reference

1. Adachi, Y., Unjoh, S. and Kondoh, M. "Development of a Shape Memory Alloy Damper for Intelligent Bridge Systems," Proceedings of the International Symposium on Shape Memory Materials, Kanazawa, Japan, 1999, pp. 31-34.
2. Choi, E. Seismic analysis and retrofit of Mid America bridges, Dept. Civil and Environmental Engineering. Georgia Institute of Technology. Atlanta, GA, USA, 2002.
3. DesRoches, R. and Fenves, G.L. "New Design and Analysis Procedures for Intermediate Hinges in Multiple- Frames Bridges," Report No. UCB/EERC-97/12, Earthquake Engineering Research Center, University of California, Berkeley, CA., December, 1997.
4. DesRoches, R. and Delemont, M., Seismic retrofit of simply supported bridges using shape memory alloys. Engineering Structures, 2002, 24:325-332.
5. DesRoches, R., McCormick, J. and Delemont M. "Cyclic Properties of Superelastic Shape Memory Alloy wires and Bars," *Journal of Structural Engineering*, ASCE, Vol. 130, No. 1, January, 2004, pp. 38-46.
6. Dolce, M., Cardone, D. and Marnetto, R., Implementation and testing of passive control devices based on shape memory alloys. Earthquake Engineering and Structure Dynamics, 2000, 29: 945-968.
7. Graesser E.J. and Cozzarelli F.A., "Shape memory alloys as new materials for aseismic isolation," *Journal of Engineering Mechanics*, ASCE, 1991, 117(11): 2590-608.
8. Ocel J., DesRoches, R., Leon, R.T., Hess, W.G., Krumme, R., Hayes, J.R. and Sweeney, S. "Steel Beam Column Connections Using Shape Memory Alloys," *Journal of Structural Engineering*, ASCE, Vol. 130. No. 5, May, 2004, pp.732-740.
9. Prakash, V., Powell, G.H., Campbell, S.D. and Filippou, F.C., DRAIN 2DX User Guide, Department of Civil Engineering, University of California at Berkeley, 1992.
10. Wen, Y.K. and Wu, C.L. "Uniform Hazard Ground Motions for Mid-America Cities," Earthquake Spectra, Vol. 17, No. 2, 2001, pp. 359-384.
11. Wilde K. Gardoni, P. and Fukino Y. "Base isolation system with shape memory alloy device for elevated highway bridges," Engineering Structures 22, 2000, pp. 222-229.